STP 1220

Fracture Mechanics: 25th Volume

Fazil Erdogan, Editor

ASTM Publication Code Number (PCN):
04-012200-30

ASTM
1916 Race Street
Philadelphia, PA 19103
Printed in the U.S.A.

Jian-Sheng Wang[1] and Glenn E. Beltz[2]

ON THE DIRECTIONALITY OF INTERFACIAL CRACKING IN BICRYSTALS AND THE LOADING PHASE ANGLE DEPENDENCE

REFERENCE: Wang, J.-S. and Beltz, G. E., "**On the Directionality of Interfacial Cracking in Bicrystals and the Loading Phase Angle Dependence,**" Fracture Mechanics: 25th Volume, ASTM STP 1220, F. Erdogan, Ed., American Society for Testing and Materials, Philadelphia, 1995.

ABSTRACT: Experimental evidence on the direction and loading phase angle dependence of interfacial cracking in bicrystals of Cu and Fe-Si alloys, and in metal/sapphire bimaterial systems, is presented. The response of a stressed interfacial crack depends not only on the structure of the interface, but also on the direction of the crack propagation and the local loading conditions. This directionality of interfacial cracking and the loading phase angle effect seem explainable in terms of the competition between dislocation emission from the crack tip and decohesion of the interface, and relate to the asymmetrical angular orientation of slip planes relative to the interface.

KEYWORDS: interfacial cracking, dislocation emission, decohesion, phase angle, directionality, ductile versus brittle transition.

The interfacial cracking behavior for a given interface between solids may depend on the direction of the crack propagation. *I. e.*, a crack may propagate in a ductile manner in one direction, while in the opposite direction it may cleave leading to brittle decohesion. Thus, the response of a stressed interfacial crack tip is not only structurally dependent, it is also directionally dependent.

The directionality of interfacial cracking in bicrystals was first quantified by the modified Rice-Thomson model[1] and supported by Wang and Anderson's experimental results on $\Sigma 9$ [110]/($2\bar{2}1$) copper bicrystals

[1]Senior Research Associate, Division of Applied Sciences, Harvard University, Cambridge, MA 02138.

[2]Assistant Professor, Department of Mechanical and Environmental Engineering, College of Engineering, University of California, Santa Barbara, CA 93106.

[2]. With the intent of extending the R-T model to the behavior of interfacial cracks in dissimilar materials, Rice, Suo and Wang [3] predicted that this directionality occurs also in bimaterials. A remarkable result of that prediction is that the ductile direction under mode I loading in the copper bicrystal mentioned above is the brittle direction in a bend test in the copper/sapphire bimaterial system when the copper $(2\bar{2}1)$ plane is bonded to sapphire. This prediction was recently verified experimentally[4] and the change of the directional behavior may be attributed to the effect of the loading phase angle[3].

In this paper, new experimental evidence of the directional dependence of corrosion fatigue in Fe-Si alloy bicrystals is presented along with a collection of published information. In order to understand these phenomena, analyses of crack tip fields in crystals [5,6] are reviewed and followed by a discussion of crack tip plasticity and the energetics of dislocation emission from the tip of an interfacial crack, so that a possible interpretation may be achieved.

EXPERIMENTAL EVIDENCE

Interfacial Fatigue Cracking in Copper Bicrystals

In a study of the fatigue behavior of Cu bicrystals contaminated with sulphur or bismuth, the $\Sigma 9$ $[110]/(2\bar{2}1)$ symmetric tilt bicrystal showed the directional dependence of crack propagation [2]. The bicrystal was first uniformly strain hardened by fatigue in a way that would not form persistent slip bands[7, 8]. It was then divided into two specimens and a notch was made by spark erosion along the boundary with the tip parallel to the [110] and co-planar with the $(1\bar{1}1)$ or $(11\bar{1})$ slip planes. The notches were cut so that in one specimen the crack would potentially propagate in the $[1\bar{1}4]$ direction, while in the other, in the opposite direction, $[11\bar{4}]$. The two notched specimens were tested by tension-compression fatigue with R = -1.

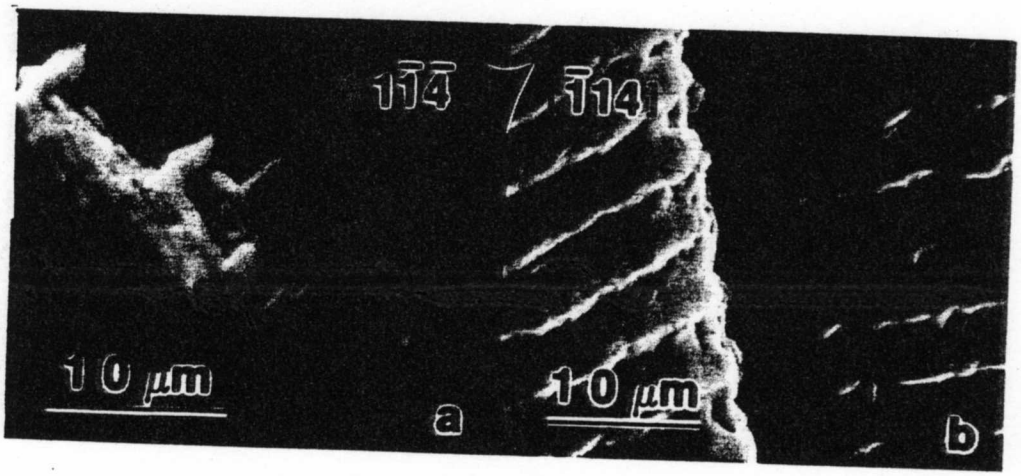

Fig.1 The fracture surfaces of the $\Sigma 9$ $[110]/(2\bar{2}1)$ Cu bicrystals. a), Cracking in the $[1\bar{1}4]$ direction and b), cracking in the $[11\bar{4}]$ direction. The arrow indicates the cracking direction.

At the resolved shear stress of 28 MPa, unstable crack propagation along the interface of the specimen with the cracking direction of $[\bar{1}14]$ occurred at 6×10^3 cycles. An intergranular brittle fracture surface with cleavage tongues was obtained (Fig.1a) and sulphur-bearing particles were observed on the fracture surfaces. In contrast, the specimen with the potential cracking direction of $[\bar{1}14]$ underwent stable fatigue cracking for 6.5×10^4 cycles without fracture. It was then broken at a monotonic tensile loading corresponding to a resolved shear stress of 76.7 MPa. The fracture surfaces showed a well developed striation structure (Fig.1b). No sulphide particles were found on the fracture surface, indicating a transgranular fracture. Since the only difference between these two specimens is the directions of crack propagation, the different behaviors can only be interpreted as the directional dependence of the ductile versus brittle response of the interface.

Fracture Behavior of Copper/Sapphire Interfaces

In the spirit of testing the idea that the competition between dislocation emission and cleavage decohesion controls the ductile versus brittle behavior of a metal/ceramic interface and that the crack tip response is directionally dependent, Wang and Beltz[4] studied the fracture behavior of a copper/sapphire interface.

Rectangular pieces of Cu single crystals were cut via EDM with the basal surfaces parallel to $(2\bar{2}1)$ or (001) crystallographic planes and the side surfaces parallel to (110) planes. The $(2\bar{2}1)$ or (001) surface was bonded to the basal plane or $(11\bar{2}0)$ plane of a commercially-obtained sapphire slide by diffusion bonding. TEM examination showed that there was no intermediate interaction layer in the interface and good atomic bonding was achieved [9]. A pre-notch was made at the midpoint of the

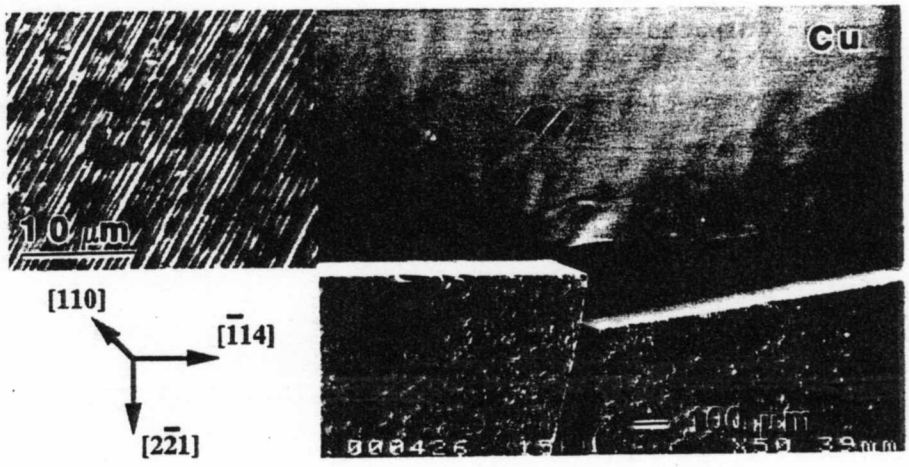

Fig.2. Side view of a Cu/sapphire specimen after 4-point bending test showing decohesion in the $[\bar{1}14]_{Cu}$ direction and blunting in the $[\bar{1}14]_{Cu}$ direction. The attached photo shows slip traces in Cu near the crack-tip region of the $[\bar{1}14]_{Cu}$ direction.

sapphire layer and then the specimen was subjected to a bend load to initiate an interfacial crack. The pre-cracked specimen was loaded under four-point bending until a nonlinear load versus deflection relation was noted and then was unloaded and reloaded several times to let the crack grow.

In all but one of the six Cu(2$\bar{2}$1)/sapphire specimens tested, the interfacial crack propagated only in the $[\bar{1}14]_{Cu}$ direction causing interfacial debonding, while plastic deformation occurred in the opposite direction, $[114]_{Cu}$, as shown in Fig.2. In one specimen the crack propagated in the $[\bar{1}14]_{Cu}$ direction a small amount, but in the $[\bar{1}\bar{1}4]_{Cu}$ direction an unstable cracking occurred causing half the sapphire layer to detach entirely from the copper crystal. On the $(110)_{Cu}$ side surface, dense slip traces appeared near the tip area in the $[\bar{1}14]_{Cu}$ direction, while in the opposite direction the slip traces were much less. The results showed a strong directional dependence of interfacial cracking in the Cu(2$\bar{2}$1)/sapphire interface. The interface was brittle in the $[\bar{1}14]$ direction and ductile in the $[1\bar{1}4]$ direction, opposite to that in the Σ9 [110]/(221) bicrystals. This directional dependence did not appear in the Cu(001)/sapphire specimens. There, the interfacial crack grew in both directions by debonding and deformation. Slip traces were observed on the $(110)_{Cu}$ surfaces near both crack tips.

Corrosion Fatigue in Fe-2.7wt.%Si Bicrystals

Fe-Si bicrystals are known to be susceptible to intergranular corrosion fatigue [10] and stress corrosion cracking (SCC) in $(NH_4)_2CO_3$ and $(Na_2CO_3+NaHCO_3)$ solutions [11]. The processes of corrosion fatigue and SCC were described by a simple slip step dissolution model, in which crack growth is assumed to proceed by alternate dislocation slip and film rupture and dissolution. A directional dependence of crack growth might thus be anticipated when there is an asymmetry of dislocation activity at opposite crack tips.

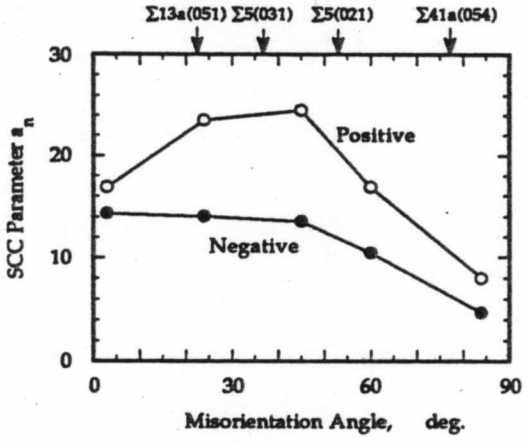

Fig.3. The IGSCC propensity vs. the tilt angle for symmetrical [010]-tilt bicrystals for cracking in the opposite directions. (by courtesy of Vehoff *et.al.* [11].)

In a study of the influence of localized slip on the nucleation and growth of intergranular stress corrosion cracking (IGSCC), Vehoff et. al. found a directional effect upon IGSCC in [010] symmetric tilt bicrystals of an Fe-2.7wt.%Si alloy [11]. Their results are replotted in terms of a brittleness parameter, $a_n = \mathrm{Cot}(\alpha/2)$, where α is the crack tip opening angle, versus the tilt angle of the bicrystal in Fig.3. A higher value of a_n represented samples more susceptible to IGSCC. The authors believed that the cracking directional dependence was due to the asymmetry of the shear stresses on the active slip planes near the crack tip in opposite directions.

The directional dependence of corrosion fatigue and SCC was studied in detail with Σ5[100]/(021) bicrystals of an Fe-2.7wt.% Si alloy [12]. Single edge cracked tension specimens (SECT) in dimensions of 5 × 6 × 30 mm were cut by EDM to allow the interface to be perpendicular to the specimen axis. Notches were made along the boundaries in opposite directions, $[0\bar{1}2]$ and $[01\bar{2}]$, respectively. For convenience, the $[0\bar{1}2]$ direction was designated the positive direction and $[01\bar{2}]$, the negative. Fatigue and SCC tests were carried out in a standard three-electrode cell in a solution of 2M $(NH_4)_2CO_3$ at 343 K under potentiostatic control.

Fatigue corrosion tests were conducted under a constant load control model with the initial ΔK_I = 6.5 MPa$\sqrt{m}$, at the mean level of 7 MPa$\sqrt{m}$ and the load frequency 1 Hz. The specimen with a positive crack failed at 6×10^3 cycles. Figure 4a shows the fatigue fracture surface with striations in the [412] and $[41\bar{2}]$ directions and secondary cracks along (100) cleavage planes. Slip bands in spacing of about 100 μm along the [012] direction were observed on the (100) surface. They were identified to originate from the (121)[111] slip system. Slip bands along the [011] direction were also found on the side surface, suggesting (211) or (011) systems were also activated during fatigue. In contrast, almost no crack propagation was detected after 3×10^4 cycles for the specimen with negative crack. The specimen finally cleaved along the (010) cleavage plane under a monotonic loading at K_{IC} = 27 MPa$\sqrt{m}$

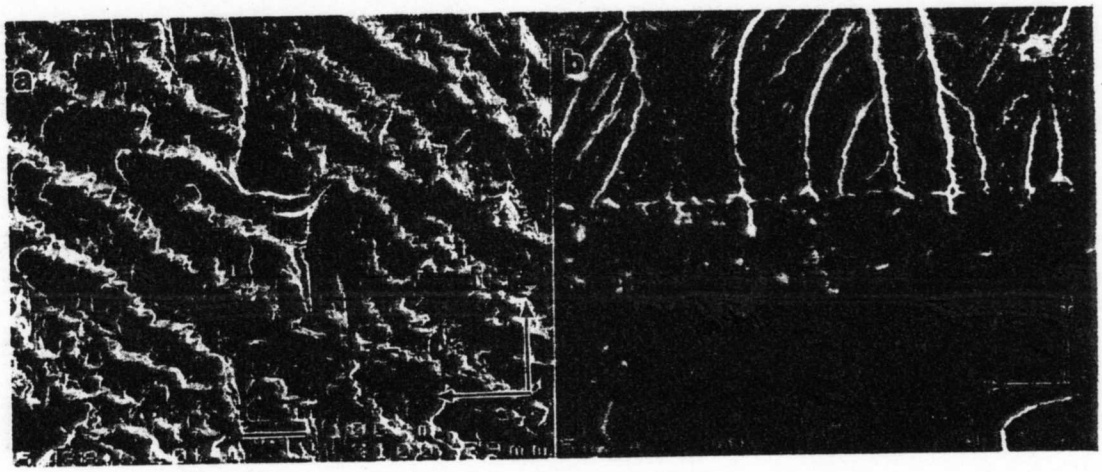

Fig.4. The fracture surfaces of the Σ5[100]/(021) bicrystals after corrosion fatigue. a), Cracking in the positive direction, fatigue striations are shown, and b), in the negative direction, cleavage.

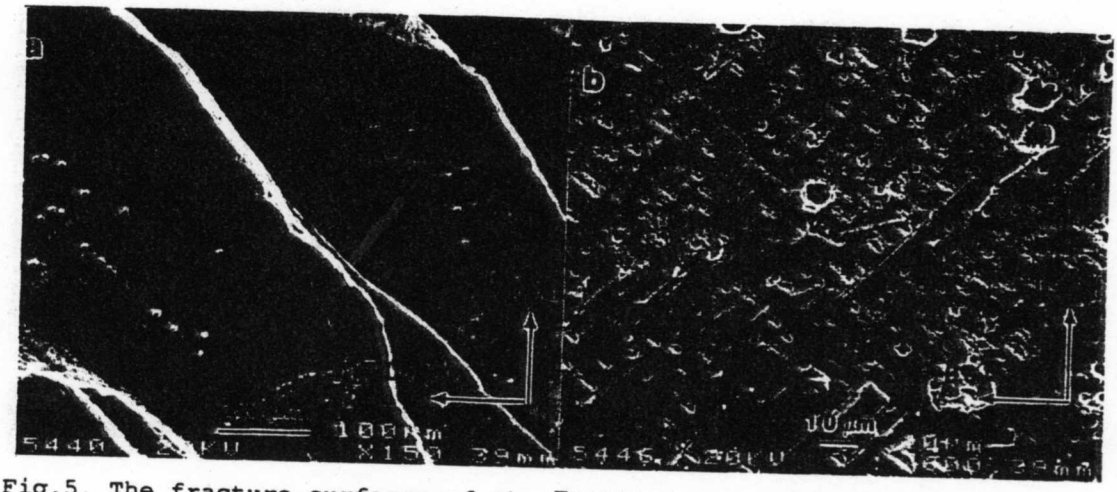

Fig.5. The fracture surfaces of the Σ5[100]/(021) bicrystals after SCC plus corrosion fatigue. Cracking in the positive, a), and negative, b), directions.

(Fig. 4b). Minimal [012] slip traces were found on the (100) side surface of the specimen accompanying the cleavage. No slip traces originating from (211) or (011) slip systems were detected.

Repeated sustained and cyclic loading tests were conducted at a sustained tension of 5700 N (initially K_I = 18 MPa$\sqrt{m}$) for 1.8×10^3 seconds followed by fatigue in load control model at initial K_{Imax} = 16 MPa $m^{1/2}$ for 300 cycles. The specimen with a positive crack, [01$\bar{2}$], failed after two successions of sustained plus cyclic loadings when the maximum value
of K_I reached about 44 MPa$\sqrt{m}$. Figure 5a shows striations developed during the second course of fatigue. In contrast, the specimen with a negative crack failed at K_I = 27 MPa $m^{1/2}$ by cleavage along (010) during sustained loading without detectable crack propagation (Fig.5b). No slip traces were found on the (100) side surface.

CRACK TIP PLASTICITY IN CRYSTALS

In all cases tested, extensive plastic deformation near the crack tip area, especially in the ductile direction, occurred, indicating that dislocation slip from internal sources was involved. The asymmetry of the plastic behaviour near the tips in opposite directions may thus be responsible for the directional dependence observed. The directionality of interfacial cracking behavior in Cu bicrystals [5], Fe-Si alloy bicrystals [6], and Cu/sapphire bimaterials [6] has been examined with asymptotic and finite element methods for stationary cracks in ideally plastic and strain hardening single crystals from a small strain continuum mechanics point of view. A brief summary of the results is presented.

The asymptotic solutions are based on the results of Rice and his colleagues [13, 14] that the near tip field for stational cracks is divided into angular sectors around the crack tip with boundaries

located along traces of slip planes or perpendicular to these traces, and stress and shear displacement discontinuities occur at sector boundaries. The possible shearing mode changes from sector to sector depending on whether the concentrated shearing zone is parallel or perpendicular to the corresponding slip plane. A regular shearing corresponding to the zones parallel to a slip plane can be accomplished by dislocation glide along the slip plane. When the zone is perpendicular to the active slip plane a kink-like mode must be involved, which requires dislocation dipoles nucleated from internal sources. When the number of dislocation sources is limited (e.g., in the case of our strain hardened Cu bicrystals) or formation of dipoles is difficult (e.g., in the Fe-Si alloy) dislocation slip might be pinched resulting in brittle fracture. Saeedvafa [5] and Mesarovic's [6] results show that in the Cu and Fe-Si alloy bicrystals studied, immediately ahead of the tip two different deformation mechanisms are operational in opposite directions. The ductile direction in the Cu bicrystals and the corrosion-fatigue insensitive direction (which may also be called the ductile direction as discussed later) in the Fe-Si alloy bicrystals corresponds to a regular shearing, while the brittle direction or the corrosion fatigue sensitive direction corresponds to the kink type shearing.

The finite element analyses for simulating the behavior of the Cu and Fe-Si alloy bicrystals tested were based on the Hill and Rice crystal plasticity constitutive theory [15], as formulated by Asaro and Rice [16], with the infinitesimal deformation and weakly rate dependent assumptions. A 'User Material' subroutine [17] was used in the finite element code ABAQUS to incorporate single crystal plasticity laws. For the Cu bicrystals the slip system is {111}<110> and for Fe-Si alloy bicrystals two families of slip systems, {121}<111> and {110}<111>, are active and the critical resolved shear stresses for the two types of slip systems were assumed to be equal [18]. The general observations of the finite element analyses are summarized as follows.

i. The tensile stress ahead the crack tip is essentially the same for both directions.

ii. The overall plastic zone size is larger in the ductile direction than that in the brittle direction.

iii. The zone of intense plastic deformation leans forward in the ductile direction, but backward in the brittle direction.

The last observation of the finite element analyses is essential in understanding the directional dependence in the bicrystals tested under cyclic loading conditions as discussed in [19]

ENERGETICS OF DISLOCATION EMISSION FROM THE CRACK TIP

The directionality of interfacial cracking may be understood in terms of the competition between dislocation emission from the crack tip and decohesion of the interface, as proposed by Armstrong [20] and Kelly, Tyson and Cotrell [21] in the 1960's and later modelled by Rice and Thomson [22] and recently advanced by Rice *et.al.* [1, 3, 23, 24]. In the model, the critical energy release rate for dislocation emission from the crack tip, G_{disl}, and the critical energy release rate for

cleavage, G_{cleav}, were compared. If $G_{disl} < G_{cleav}$ dislocations were assumed to emit from the crack tip, blunting the tip, before interfacial decohesion. The interface was predicted to be intrinsically ductile. If, on the other hand, $G_{disl} > G_{cleav}$, decohesion was assumed to occur before dislocation emission and the interface was intrinsically brittle. While G_{cleav} is relatively insensitive to the misorientation of the crystal involved [3], G_{disl}, being mainly determined by the resolved shear stress on the slip plane, may change dramatically with the changing of the inclination angle of the slip plane with respect to the interface. Due to the geometrical asymmetry of the slip plane configurations at the crack tip in opposite directions, the critical energy release rate for dislocation emission from the crack tip in opposite directions may differ significantly.

The critical energy release rate for dislocation emission from a crack tip along an interface can be obtained based on a continuum dislocation mechanics approach, the Rice-Thomson type approach, or a new approach of the Peierls-Nabarro type, which treats the process of incipient dislocation nucleation from a crack tip based on the Peierls-Nabarro concept. A brief description of these two approaches is given in the Appendix.

Dislocation Nucleation and Emission from the Crack Tip in Copper Bicrystals

The critical mode I G_{disl} for dislocation nucleation in Cu bicrystals as a function of the slip plane inclination angle θ is calculated with the R-T type model. In the calculations, the core cutoff is assumed to equal the Burgers vector, the ledge energy per unit area created by dislocation emission is taken to be one tenth of the surface free energy of Cu [2] and an isotropic elasticity is presumed.

For [110] symmetric tilt bicrystals, where the crack front lies along the tilt axis, the likely dislocations to be activated are the partial dislocations with $\boldsymbol{b} = a\langle 112\rangle/6$ and $\phi = 60°$ and then $\phi = 0°$ or the perfect dislocation with $\phi = 30°$. As discussed in [2] the critical

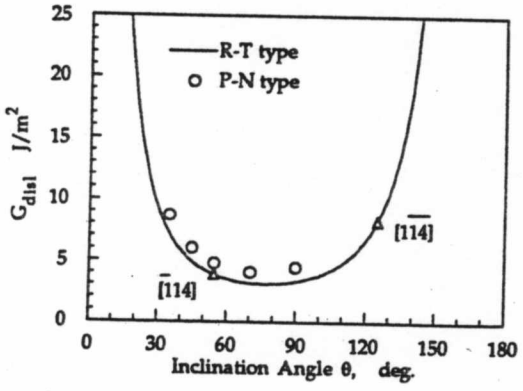

Fig.6. The critical mode I G_{disl} vs. θ in Cu bicrystals. The opposite directions in the $\Sigma 9$ [110]/(221) bicrystals tested are indicated.

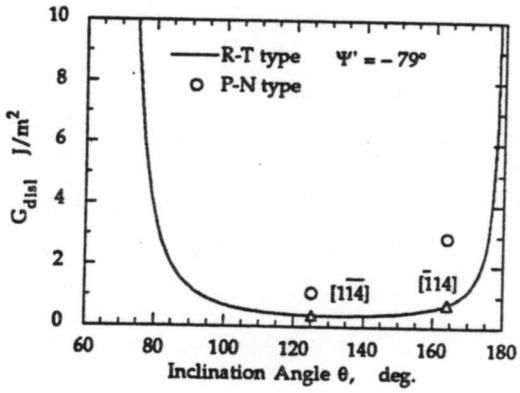

Fig.7. The critical G_{disl} vs. θ for Cu/sapphire interfaces loaded in pure bend. The opposite directions tested are indicated.

energy release rate for dislocation emission is determined by the minimum value of G_{disl} required to nucleate the partials with $\phi = 60°$. The results are shown in Fig.6. In the figure results from the P-N type model (which neglects tension-shear coupling and takes γ_{us} = 0.22 J/m^2 for Cu) are also displayed, which predicts the same G_{disl} vs. θ relation.

The directionality observed in Σ9 [110]/(2$\bar{2}$1) copper bicrystals might be understood by comparing predictions for opposite cracking directions. For cracking in the [1$\bar{1}$4] direction, the most likely dislocations to be activated are partials on the (1$\bar{1}$1) slip plane with θ = 54.7°, $\phi = 60°$ and G_{disl} = 3.8 J/m^2. If the crack growth direction is reversed, in the [1$\bar{1}$4] direction, the most active slip systems remain the same, but in this case, $\theta = 125.3°$ and the predicted value of G_{disl} is 8.3 J/m^2, more than twice that of the [1$\bar{1}$4] direction. Dislocation emission is preferred in the [1$\bar{1}$4] direction.

Dislocation Nucleation and Emission from the Interfacial Crack Tip in Copper/Sapphire Bimaterials

For the Cu/sapphire bimaterial system under the pure bend conditions the atomic scale phase angle is -79° [3]. Assuming the sapphire is purely elastic and dislocations can only be activated in Cu, the critical energy release rate for dislocation emission from the $[110]_{Cu}$ crack-tip vs. θ is presented in Fig.7. Several observations follow:

i. Similarly to the bicrystal behavior, G_{disl} is a strong function of θ with a minimum, but due to the mostly mode II loading conditions for the bimaterials the minimum value occurs at a larger θ angle.

ii. The minimum value of G_{disl} for the bimaterials is much lower than that for bicrystals, indicating a toughening effect of the interfacial crack by a rigid solid.

iii. The active slip systems have changed from the (1$\bar{1}\bar{1}$) slip plane with $\boldsymbol{b} = a[211]/6$ or $a[1\bar{2}1]/6$ and $\phi = 60°$ to the (1$\bar{1}$1) slip plane with $\boldsymbol{b} = a[121]/6$ or $a[2\bar{1}1]/6$ and $\phi = 60°$. In this case the θ angle is 125.3° for cracking in the [1$\bar{1}$4] direction and 164.2° for cracking in the [1$\bar{1}$4] direction, respectively. In contrast with bicrystals, G_{disl} for cracking in the [1$\bar{1}\bar{4}$] direction is two times lower than that for cracking in the [1$\bar{1}$4] direction and this may partially explain the directional dependence observed in the Cu/sapphire system.

The difference between G_{disl} in two opposite directions predicted by the R-T type model is not significant numerically, however. A check from the P-N type calculations is needed. Results based on those in [25] for a simplified set of slip plane constitutive relations for copper are now summarized. For the partials with $\phi = 60°$ G_{disl} = 1.08 J/m^2 when cracking in the $[1\bar{1}\bar{4}]_{Cu}$ direction and G_{disl} = 2.91 J/m^2 when cracking in the $[1\bar{1}4]_{Cu}$ direction (here, effects of tension-shear coupling are not included.) There is a difference of more than a factor of two in G_{disl} for crack growth in the opposing directions as shown in Fig.7; hence, it

is concluded that dislocation nucleation is preferred in the $[\overline{1}\overline{1}4]_{Cu}$ direction, and blunting should be favored in this growth direction.

The tension-shear coupling reduces the critical energy release rate for dislocation nucleation as shown in Fig.8, where the applied energy release rate G/γ_{us} is plotted as a function of the atomic shear displacement δ_r^{tip}/b for the $\phi = 0°$ partials for the two angles of interest. Here $\delta_r \equiv u_1^{(+)}-u_1^{(-)}$ denotes the displacement discontinuity on a mathematical cut coincident with the slip plane. The critical value for dislocation nucleation occurs at the maximum in the G/γ_{us}~δ_r^{tip}/b curve. For cracking in the $[\overline{1}\overline{1}4]_{Cu}$ direction, *i.e.*, $\theta = 125.3°$, unstable nucleation of the partial dislocation occurs at $G/\gamma_{us} = 1.839$ for $p = 0$ and $G/\gamma_{us} = 1.715$ for p = 0.1. When cracking in the $[\overline{1}14]_{Cu}$ direction, *i.e.*, $\theta = 164.2°$, instability occurs at $G/\gamma_{us} = 12.55$ for $p=0$ and $G/\gamma_{us} = 11.69$ for $p = 0.1$.

The switch of the active slip systems or the reverse of the cracking directionality in the Cu/sapphire specimens is attributable entirely to the phase angle effect. Here, the atomic scale phase angle ψ' is -79° versus 0° for mode I loading in a symmetric tilt bicrystal. The phase angle effect is shown in Fig.9, which gives G_{disl} vs. ψ' for the various slip plane inclination angles. The solid lines correspond to angles associated with the $[\overline{1}14]_{Cu}$ direction, and the dashed lines correspond to angles associated with the $[\overline{1}\overline{1}4]_{Cu}$ direction. Comparison of the curves at $\psi' = 0$ and $\psi' = -79°$ shows that the favored direction for dislocation emission reverses when the phase angle is altered.

It is not surprising that the specimens with the $(001)_{Cu}$/sapphire interface did not show directional dependence, since configurations of slip systems at the crack-tips in opposite directions are symmetric.

Dislocation Nucleation and Emission from the Crack-Tip in Iron Bicrystals

For [100] symmetric tilt Fe bicrystals the likely dislocations to be activated from the crack-tip lying along [100] might be those with $b = a\langle 111\rangle/2$ and $\phi = 35.26°$ on {110} planes. The critical mode I G_{disl} vs.θ curve predicted by the R-T type model is presented in Fig.10. Here, the core cutoff $r_o = 2/3\ b$, the ledge energy $\gamma_{ledge} = .4\gamma_s$[2] and an isotropic elasticity is presumed. Results from the P-N type model, where $\gamma_{us} \cong 0.55$ J/m^2 for Fe is assumed, are also shown in the figure. The trends predicted by both models are the same, though the P-N type model predicts a lower value for dislocation emission.

For the Σ5[100]/(021) bicrystals with the macroscopic crack front lying along [100], the coplanar slip systems are $(01\overline{1})[\overline{1}11]$, $(01\overline{1})[111]$, $(011)[\overline{1}11]$ and $(011)[111]$ When the crack propagates in the negative direction, $[0\overline{1}2]$, the active slip plane would be $(01\overline{1})$ with $\theta = 71.57°$ and $G_{disl} = 6.3$ J/m^2, as predicted by the model. In the positive direction, [012], the active slip plane (if it could ever be activated) would still be (011), but in this case $\theta = 108.43°$ and $G_{disl} = 9.6$ J/m^2, about twice that in the $[0\overline{1}2]$ direction. The model predicts that dislocations are easier to emit from the crack-tip when cracking in the $[0\overline{1}2]$ direc-

tion, which is insensitive to corrosion fatigue, than that in the opposite direction, which is corrosion fatigue sensitive.

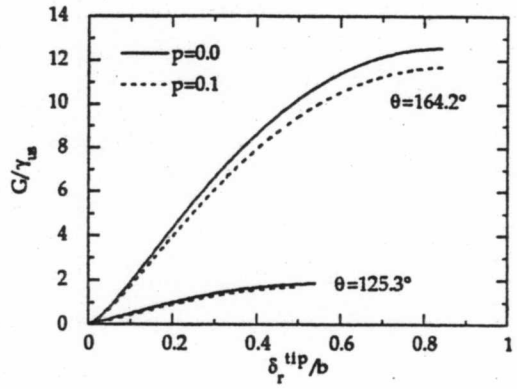

Fig.8. The applied energy release rate vs. the amount of slip at the crack tip for the two angles of interest. Effects of tension-shear coupling are shown.

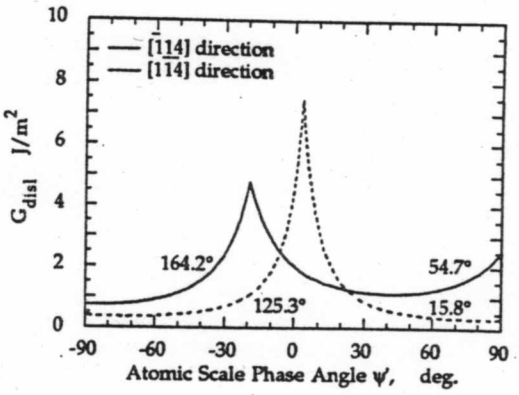

Fig.9. G_{disl} vs. ψ' for Cu/sapphire bimaterials. The numbers attached are the inclination angles θ of the potentially active slip planes.

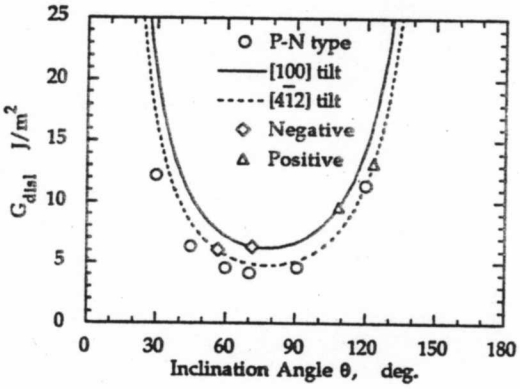

Fig.10. The mode I G_{disl} vs. θ in Fe bicrystals. G_{disl} for the $\Sigma5[100]/(021)$ bicrystals cracking in the opposite directions are marked.

Microscopically, the crack front, as observed in our tests, was zigzagged along $[4\bar{1}2]$ and $[41\bar{2}]$ (Fig.5) and the cracking direction was $[5\bar{1}2]$ or $[51\bar{2}]$, perpendicular to the crack front, for the corrosion fatigue sensitive direction. Correspondingly, the coplanar slip systems were $(1\bar{2}1)[111]$ or $(12\bar{1})[111]$, and the angle between the Burger's vector and the normal to the crack front is $\phi = 22.21°$, as if we have had a $[4\bar{1}2]$ or $[41\bar{2}]$ tilt bicrystal. Assuming isotropic elasticity and a zero atomic scale phase angle, the G_{disl} vs. θ relation for the $[4\bar{1}2]$ tilt bicrystals is plotted in Fig.10 as a dashed curve. Compared with the solid curve, it shows that dislocations are more active in {112} type slip systems than in {110} type slip systems. This may partially explain the microscopic deviation of the cracking direction observed in the

specimens. In this case, when the $(12\bar{1})[\bar{1}\bar{1}\bar{1}]$ or $(\bar{1}2\bar{1})[111]$ slip system is activated, $\theta = 123.21°$ and $G_{disl} = 13.2$ J/m^2 for the positive direction, but $\theta = 56.79°$ and $G_{disl} = 6.0$ J/m^2 for the negative direction. Dislocations are predicted to nucleate more easily in the negative direction than in the positive direction, consistent with the experimental observations that the positive direction is sensitive to corrosion fatigue, while the negative direction is insensitive. A detailed analysis will appear in work in progress [19].

CONCLUSION

1. A directional dependence of crack growth in bicrystals of fcc and bcc metals, and in bimaterials, as well as effects of the atomic scale phase angle were experimentally observed.
2. The observations are consistent with asymptotic and finite element analyses of the plastic behaviors near the crack tip region in bicrystals tested.
3. The cracking directionality and phase angle effects may be understood in terms of the competition between cleavage decohesion of the interface and dislocation emission from the crack tip.

ACKNOWLEDGEMENT

This work was supported by DARPA through the University Research Initiative Program, coordinated by University of California at Santa Barbara and NSF through the MRL at Harvard. JSW is grateful to B. Schaff with the Max-Planck Institut für Eisenforschung GmbH for providing him with Fe-2.7%Si bicrystals. Conversations with Professors A.G. Evans, J.R. Rice, Z. Suo, and D.M. Stump are gratefully acknowledged. We would like to thank Doug Galpin for proofreading the manuscript.

REFERENCES

[1] Anderson, P.M. and Rice, J.R., Scripta metallurgica Vol. 20, 1986, pp. 1467-1472, and Anderson, P.M., "Ductile and Brittle Crack Tip Response", Ph.D. thesis, Harvard University, Cambridge, Mass.,1986.

[2] Wang, J.-S. and Anderson, P.M., Acta metallurgica et materialia Vol. 39, 1991, pp. 779-792.

[3] Rice, J.R., Suo, Z. and Wang, J.-S., Metal-Ceramic Interfaces, Acta Scripta Metallurgica Proceedings Series, Vol. 4, edited by M. Rühle, A.G. Evans, M. F. Ashby, and J.P. Hirth, Pergamon Press, Oxford, 1990, pp. 269-294.

[4] Wang, J.-S. and Beltz, G.E., Structure and Properties of Interfaces and Materials, edited by Clark, W.A.T., Dahmen, U., and Briant, C.L., Proceeding of Materials Research Society, Vol. 238, Materials Research Society, Pittsburgh, 1992, pp. 405-410, Beltz, G E. and Wang, J.-S., Acta metallurgica et materialia, Vol. 40, 1992, pp. 1675-1683.

[5] Saeedvafa, M., Mechanics of Materials, Vol. 13, 1992, pp. 295-311.
[6] Mesarovic, S., work in progress.
[7] Buchinger, L., and Laird, C., Materials Science and Engineering, Vol. 76, 1985, pp. 71-76.
[8] Yan, B. and Laird, C., Materials Science and Engineering, Vol. 80, 1986, pp. 59-64.
[9] Kim, M.J., private communication.
[10] Waltersdorf, J., and Vehoff, H., Scripta metallurgica, Vol. 23, 1989, pp. 513-518.
[11] Vehoff, H., Stenzel, H. and Neumann, P., Zeitschrift für Metallkunde, Vol. 78, 1987, pp. 550-558.
[12] Wang, J.-S., unpublished work.
[13] Rice, J.R., Mechanics of Materials, Vol. 6, 1987, pp. 714-735.
[14] Rice, J.R., Hawk, D.E., and Asaro, R.J., International Journal of Fracture, Vol. 42, 1990, pp. 301-321.
[15] Hill, R., and Rice, J.R., Journal of Mechanics and Physics of Solids, Vol. 20, 1972, pp. 401-413.
[16] Asaro, R.J., and Rice, J.R., Journal of Mechanics and Physics of Solids, Vol. 25, 1977, pp. 309-338.
[17] Huang, Y., A user-material subroutine incorporating single crystal plasticity in ABAQUS finite element program, MECH-178, Harvard University, Division of Applied Sciences, 1991.
[18] Orlans-Joliet, B., J.H. Driver and Montheillet, F., Acta metallurgica et materialia, Vol. 38, 1990, pp. 581-594.
[19] Wang, J.-S.and Mesarovic, S., work in progress.
[20] Armstrong, R.W., Materials Science and Engineering, Vol. 1, 1966, pp. 251-256.
[21] Kelly, A., Tyson, W. and Cottrell, A., Philosophical Magazine, Vol. 15, 1967, pp. 567-586.
[22] Rice, J.R. and Thomson, R., Philosophical Magazine, Vol. 29, 1974, pp. 73-97.
[23] Rice, J.R., Journal of the Mechanics and Physics of Solids, Vol. 40, 1992, pp. 239-271.
[24] Rice, J.R., Beltz, G E. and Sun, Y., Topics in Fracture and Fatigue, edited by A.S. Argon, Springer-Verlag, 1992, pp. 1-58.
[25] Beltz, G. E. and Rice, J.R., Acta metallurgica et materialia, Vol. 40, 1992, pp. S321-S331.
[26] Rice, J. R., Fundamentals of Deformation and Fracture (Eshelby Memorial Symposium), edited by Bilby, B.A. Miller, K.J. and Willis, J.R., Cambridge University Press, 1985, pp. 33-56.
[27] Bacon, D.J., Barnett, D.M., and Scattergood, R.O., Progress in Materials Science, Vol. 23, 1979, pp. 51-265.
[28] Cao, H. and Rice, J.R., Journal of the Mechanics and Physics of Solids, Vol. 37, 1989, pp. 155-174.
[29] Argon, A.S., Acta metallurgica. Vol. 35, 1987, pp. 185-196.
[30] Schoeck, G., Philosophical Magazine, Vol. A 63, 1991, pp. 111-120.
[31] Beltz, G.E. and Rice, J.R., Modeling the Deformation of Crystalline Solids: Physical Theory, Application, and Experimental Comparisons edited by Lowe, T. C. and Rollett, A.D., Follansbee, P.S. and Daehn, G.S.,TMS, 1991, pp. 457-480.
[32] Sun, Y., Ph. D. thesis, Harvard University, Cambridge, Mass., 1993.
[33] Cheung, K., Yip, S., and Argon, A.S., Journal of Applied Physics,

Vol. 69, 1991, pp. 2088-2096.
[34] Ferrante, J. and Smith, J.R., Physical Review, Vol. B 31, 1985, pp. 3427-3434.
[35] Sun, Y., Rice, J.R., and Truskinovsky, L., High-Temperature Ordered Intermetallic Alloys, edited by Johnson, L.A., Pope, D.T., and Stiegler, J.O., Proceeding of Materials Research Society, Vol. 213, Materials Research Society, Pittsburgh, 1991, pp. 243-248.
[36] Sun, Y., Beltz, G. E. and Rice, J.R., Materials Science and Engineering, Vol. A 170, 1993, pp. 67-85.

APPENDIX

The Rice-Thomson Approach

A treatment of dislocation loop emission in bimaterials and asymmetric bicrystals, analogue to that of Anderson and Rice for loop emission in symmetric bicrystals [1] and of Rice, Suo and Wang for emission of a straight line dislocation in bimaterials [3], is given. This procedure evokes a dislocation core cutoff, a poorly defined parameter in the continuum elastic dislocation theory and, in essence, it deals only with emission of dislocations from the crack tip, not dislocation nucleation.

The Rice-Thomson type approach takes into account the balance of the work done by the applied stress and the energy of a dislocation emanating from the crack tip. Considering an interface in a bimaterial system, where the crack front lies along the intersection of a slip plane and the interface, a semicircular dislocation loop is supposed to emit into material 1 from the crack tip and material 2 is assumed to be elastic, the total energy of the loop as a function of the loop radius, r, consists of three terms: the self energy of the loop, the energy of the ledge created by crack-tip blunting due to dislocation emission and the Peach-Koehler type work done by the local crack-tip stress field to expand the loop.

The near-tip stress field for an interfacial crack between dissimilar isotropic materials has the singular form [3]:

$$\sigma_{\alpha\beta} = \frac{1}{\sqrt{2\pi r}}[\mathrm{Re}\,(Kr^{i\varepsilon})\,\Sigma^{I}_{\alpha\beta}(\theta) + \mathrm{Im}\,(Kr^{i\varepsilon})\,\Sigma^{II}_{\alpha\beta}(\theta)] \qquad (\alpha,\ \beta = x,\ y) \tag{A1}$$

Here the angular functions $\Sigma_{\alpha\beta}(\theta)$ of superscripts I and II correspond to tractions across the interface at $\theta = 0$ of tensile and in-plane shear, respectively, so that the complex stress intensity factor, K, is defined, θ is the angle made by the active slip plane and the interface and ε is the oscillatory index for the material pair. For simplicity, forms for 2-D conditions are presented.

For most material pairs the parameter ε is small so that $Kr^{i\varepsilon}$ is only a weak function of r. In the case of the dislocation emission from the crack tip, for all r of order b, the Burgers vector of the loop in consideration, we have $Kr^{i\varepsilon} \cong Kb^{i\varepsilon}$. Based on this approximation, an atomic scale loading phase angle, ψ', is defined by $Kb^{i\varepsilon} = |K|e^{i\psi'}$ [3], which is related to the applied loading phase angle by

$$\psi' = \psi - \varepsilon \ln(L/b) \tag{A2}$$

where L is a characteristic length scale connected with the dimension of the specimen and by definition $\psi = \tan^{-1}[Im(KL^{i\varepsilon})/Re(KL^{i\varepsilon})$.

Once the local atomic scale phase angle is defined, one has $Re(Kr^{i\varepsilon}) \equiv |K| \cos\psi'$ and $Im(Kr^{i\varepsilon}) \equiv |K| \sin\psi'$. The resolved shear stress acting on the slip plane in the direction of the Burgers vector is thus given by

$$\tau = |K| b r^{-1/2} (S^{I} \cos\psi' + S^{II} \sin\psi') \tag{A3}$$

where $S^{I} = (2\pi)^{-1/2} \cos\phi \Sigma^{I}_{r\theta}(\theta)$ and $S^{II} = (2\pi)^{-1/2} \cos\phi \Sigma^{II}_{r\theta}(\theta)$, ϕ is the angle between the Burgers vector and the crack front normal. The Peach-Koehler force, τb, is integrated over the entire area of the semicircular loop of the dislocation [1] to obtain the work done by the applied stress

$$W_{stress} \cong 3.5 |K| b r^{3/2} (S^{I}\cos\psi' + S^{II}\sin\psi') \tag{A4}$$

Following the procedure in [1-3], the critical stress intensity factor for dislocation emission from the crack-tip is derived as

$$|K|(S^{I}\cos\psi' + S^{II}\sin\psi') = 0.76 \frac{A_o}{b} \sqrt{\frac{m}{r_o}} \exp \frac{\gamma_{ledge} b \cos\phi \sin\theta}{\pi A_o} \tag{A5}$$

where A_o is the pre-logarithmic energy factor matrix, $A_{\alpha\beta}$, for a straight dislocation line with the same Burgers vector as the loop averaged over all possible orientation angles ϕ of the line within the loop plane [26, 27], m is a geometric factor given by Gao and Rice [28], r_o is the dislocation core cutoff and γ_{ledge} is the free energy of the ledge, which is usually a fraction of the surface free energy [2]. The Irwin-type critical energy release rate for the dislocation emission is then given.

The Peierls-Nabarro Type Approach

The method for determining G_{disl} as outlined in the previous discussion treats a dislocation as an elastic singularity, with a poorly defined core cut-off parameter, that exists ahead of the crack tip prior to loading. It has been recognized, however, that a full dislocation is likely to emerge unstably from an incomplete, incipient dislocation at the tip [29, 30], and an exact treatment of this has been given recently by Rice [23]. That treatment, discussed in further detail by Beltz and Rice [25, 31], solves the elasticity problem of a traction free crack with a Peierls-type stress versus displacement relation being satisfied as a boundary condition along a slip plane ahead of a crack tip. Once this problem is solved for a suitable constitutive relation for material sliding and perhaps opening along a slip plane, there is no need for the core cut-off parameter. This method allows for the existence of an extended dislocation core during nucleation, and eliminates the uncertainty in choosing the core parameter.

The *P-N* type approach requires a knowledge of the Peierls shear stress τ versus relative atomic displacement, Δ_r, relation. This type of data has been calculated through the use of pair potentials or the embedded atom method by several researchers. The integral of such a curve from $\Delta_r = 0$ to the unstable equilibrium position, at which the shear stress next vanishes, is called the unstable stacking energy, a recently identified solid state parameter, denoted γ_{us} [23]. Atomistic calculations for the embedded atom model iron (*EAM-Fe*) give values of $\gamma_{us} = 0.517$ J/m^2 for {110}<111> slip system and 0.581 J/m^2 for {112}<111> slip system, respectively [32].

For the simplest case, *i.e.*, when the slip plane is coplanar with the crack plane, $\theta = 0$, and in the shear-only model, an elegant analytical relation for dislocation nucleation from the crack-tip can be contained by the path independent *J*-integral [23]:

$$G_{disl} = (1-\nu) K_{IIc}^2/2\mu = \gamma_{us} \tag{A6}$$

G_{disl} may be calculated for more realistic situations involving inclined slip planes and mixed mode loadings, and also for bimaterial crack tip fields; however, the above result illustrates a feature that pervades these complicated cases: the energy release rate for dislocation nucleation scales with γ_{us}.

By introducing the concept of the effective stress intensity factor, Rice [23] proposed an approximate treatment of dislocation nucleation when $\theta \neq 0$ and derived the basic nucleation condition for a complete dislocation in an isotropic material, approximately

$$|f_I(\theta)\ K_I + f_{II}(\theta)\ K_{II}|\ \cos\phi + f_{III}(\theta)\ K_{III} \sin\phi = [2\mu\gamma_{us}\ [\cos^2\phi + (1-\nu)\ \sin^2\phi]]^{1/2} \tag{A7}$$

where f's are the angular functions given by [23]. A similar treatment can be employed for anisotropic materials, for which the readers are referred to [24].

Further complexities arise when the effects of normal tractions and dilatant opening across the slip plane are included in the model. This situation occurs if a mixed mode loading is applied, or in more realistic cases, when the slip plane is inclined with respect to the crack plane. In these cases, the tensile stresses across the slip plane induce a softening effect in shear [29, 33], the τ versus Δ_r curve changes its shape and hence, the effect of superposed tension on the "effective" γ_{us}, denoted $\gamma_{us}^{(u^*)}$, must be investigated. A ratio of $\gamma_{us}^{(u^*)}/\gamma_{us} = 0.7294$ for EAM-Fe was given by Sun [32] from atomistic calculations.

An exact solution for the effect of tension normal to the slip plane was provided recently by Rice *et al.* [23, 31] by assuming a tensile stress versus the normal component of separation relation consistent with the universal binding energy relation (UBER) [34], that $\sigma = (2\gamma_s/L)\ (\Delta_\theta/L)\ exp(-\Delta_\theta/L)$, where γ_s is the surface energy, Δ_θ is the atomic opening displacement and the parameter L is the

characteristic length associated with the decohesion process. In this exact treatment, the effects of the tension/shear coupling are represented by the dilation parameter p defined by $p = \Delta_\theta^*/L$, where Δ_θ^* is the relaxed atomic opening displacement corresponding to that for vanishing normal stress at the unstable shear equilibrium position, $\Delta_r = b/2$. The embedded atom method, fit to material properties, has been employed to estimate parameters L/b, p and q ($= \gamma_{us}/2\gamma_s$), and a relaxed unstable stacking energy, $\gamma_{us}^{(r)}$, is defined. For EAM-Fe, $\gamma_{us}^{(r)}$ = 0.44 and 0.50 J/m^2 for {110}<111> and {112}<111> slip systems, respectively [32]. The energy release rate for dislocation nucleation with full σ–τ coupling can be determined numerically, which shows that results based on the effective K concept and $\gamma_{us}^{(u^*)}$ are consistent with the exact numerical solutions [32, 35, 36].